Intramolecular Quenching of Porphyrin Fluorescence by a Covalently Linked Ferrocene in DNA Scaffolding†

Nancy B. Thornton, Hania Wojtowicz, Thomas Netzel,* and Dabney W. Dixon*

Department of Chemistry, Georgia State University, Atlanta, Georgia 30303

Received: September 30, 1997; In Final Form: December 2, 1997

Intramolecular quenching of fluorescence from a cationic porphyrin by a covalently attached ferrocene in both solution and DNA is reported. Two ferrocenyl porphyrins have been prepared, tris(4-*N*-methylpyridiniumyl), mono(phenyl-OCH_2CH_2ferrocene)porphyrin, P3Fc, and *cis*-bis(4-*N*-methylpyridiniumyl), bis(phenyl-OCH_2CH_2ferrocene)porphyrin. Binding studies for P3Fc indicate that intercalation of the porphyrin moiety into DNA occurs at low ionic strength (10 mM NaCl); outside binding of the complex is favored at increased ionic strength (100 mM NaCl). The outside binding of P3Fc at high ionic strength is attributed to the hydrophobicity of the molecule, which causes it to undergo salt-induced stacking in aqueous solution. The photophysical properties of P3Fc are examined in MeOH, in phosphate buffer, and in the presence of double-stranded DNA. Efficient quenching of the photoexcited singlet state of the porphyrin by electron transfer from the appended ferrocene is observed in MeOH and buffer solutions with average rate constants of $\geq 1 \times 10^{10}$ and 9×10^9 s^{-1}, respectively. When P3Fc is intercalated into DNA, the average rate of photoinduced intramolecular electron transfer is not appreciably reduced (7×10^9 s^{-1}), suggesting that electronic coupling between the D−A pair is strong even under conditions where close contact is restricted. Assuming that for this donor−linker−acceptor complex, in which the porphyrin and ferrocene are separated by an $-OCH_2CH_2-$ spacer, intercalation of the porphyrin into DNA does not significantly reduce the electronic coupling between the donor and acceptor, the observed subnanosecond electron-transfer rates in and out of DNA show that changes in redox potentials or reorganization energy either compensate one another or have negligible kinetic consequences.

Introduction

Extensive study of photoinduced charge separation in organic and organometallic donor−acceptor molecules has revealed many of the factors that control long-distance electron transfer.[1−7] Studies are increasingly focused on electron transfer in larger structures, with the goals of understanding vectorial electron transfer in biological systems[8−12] and of designing molecular electron-transfer devices.[13−16]

The role of DNA in serving as a medium for long-distance transfer is the focus of current interest; both experimental[17−21] and theoretical[22] approaches have been reviewed recently.[23−25] Some studies have looked at electron transfer between donors and acceptors covalently bound to the DNA strands.[26−28] Other studies have focused on electron transfer between two intercalators bound to DNA.[17,21,29−31] Despite substantial experimental work, the role of the DNA itself in controlling the rate of electron transfer along the DNA helical axis is still the subject of debate.[32,33] A number of research groups have also assessed electron transfer between a DNA-bound intercalator and a donor or acceptor in solution; the field has been reviewed recently.[17] When the reagents are not covalently attached either to DNA or to one another, data analysis can be complicated by the spread of possible electron-transfer distances,[29] the possibility of cooperative binding of the donor and acceptor,[30,34] and the necessity to account for the concentration of the mobile reagent in the grooves of the DNA and the reduced diffusional dimensionality of this groove-bound reagent.[35,36]

Unimolecular electron transfer between the donor and acceptor of a covalently attached donor−linker−acceptor (D−L−A) assembly, one component of which is intercalated in the DNA duplex, provides a new approach to probe the role of the DNA in controlling electron transfer. This system is formally orthogonal to other systems studied to date, in that the direction of electron transfer is perpendicular to the DNA helical axis. Comparison of the rate of electron transfer between the donor and acceptor in solution with the rate in DNA may give additional insight into the role of the DNA as an environmental modulator of electron-transfer processes. Effects might arise from restricting the available geometries of the donor−linker−acceptor assembly, changes in the redox potential of the intercalated[37,38] or groove-bound[39−42] portion of the molecule, and changes in the reorganization energy for electron transfer.[43,44] Restricting the available conformations of the molecule in the DNA scaffold might also result in a less complicated kinetic profile for nonrigid systems.

As the first example of a donor−linker−acceptor DNA-binding molecule, we chose to synthesize the ferrocenyl porphyrin P3Fc (Figure 1) for its favorable DNA binding and photophysical properties. Tris(4-*N*-pyridiniumyl) porphyrins

† Abbreviations: TMPyP(4) = *meso*-tetrakis(4-*N*-methylpyridiniumyl)-porphyrin; P3 = tris(4-*N*-methylpyridiniumyl)(monophenyl)porphyrin; Fc = ferrocene; P3Fc = tris(4-*N*-methylpyridiniumyl), mono(phenyl-OCH_2CH_2ferrocene)porphyrin; OMP = 5,15-bis(4-tolyl)-2,3,7,8,12,13,17,18-octamethylporphyrin; hypochromicity, $H\% = [((\epsilon_f - \epsilon_b)/\epsilon_f) \times 100]$ where ϵ_f and ϵ_b are the extinction coefficients for free and bound porphyrins at λ_f and λ_b, respectively; N00 buffer = 7.5 mM NaH_2PO_4, 1 mM EDTA, pH 7.0; N10 buffer = 7.5 mM NaH_2PO_4, 1 mM EDTA, 0.1 M NaCl, pH 7.0; CT DNA, calf thymus DNA; DNA_{bp} = DNA base pairs; CD = circular dichroism.

* To whom correspondence should be addressed. Phone 404-651-3908, Fax 404-651-1416, e-mail ddixon@gsu.edu.

S1089-5647(97)03180-5 CCC: $15.00
Published on Web 02/20/1998

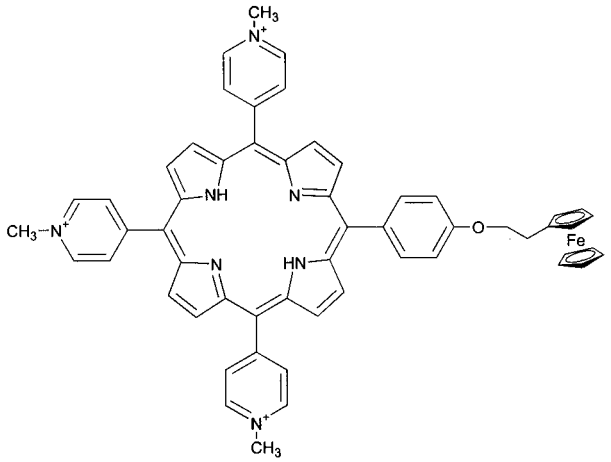

Figure 1. Structure of 5-[4-(2-ferrocenylethoxy)phenyl]-10,15,20-tris-(4-*N*-methyl-pyridinumyl)porphyrin, P3Fc.

are generally thought to be intercalators;[45−48] P3Fc would thus be expected to adopt a geometry with the porphyrin intercalated into the DNA and the ferrocene in a groove. The cationic *N*-methylpyridiniumyl porphyrins have excellent photophysical characteristics, with high extinction coefficients (approximately 2×10^5 M^{-1} cm^{-1} at the Soret maximum), suitable fluorescence quantum yields (0.01−0.05 in H_2O),[49−51] and a first excited state that lives approximately 5 ns in H_2O. Photophysical studies of a hydrophobic ferrocenyl porphyrin indicate that electron transfer (rather than energy transfer) from the ferrocene to the photoexcited porphyrin takes place even at a very moderate driving force ($\Delta G°$ approximately −0.1 eV).[52] The three cationic *N*-methylpyridiniumyl rings of P3Fc tune the driving force for electron transfer in this system to even more favorable energies; $\Delta G°$ for photoinduced electron transfer from the ferrocene to the excited porphyrin is expected to be −0.66 eV in P3Fc.

The ferrocene and porphyrin moieties in P3Fc are linked by a three-atom chain. This short linker both limits the conformational space of the ferrocene moiety with respect to the porphyrin and favors fast through-bond electron transfer. Indeed, our results indicate that electron transfer takes place with a time constant of <200 ps both in solution and when bound to the DNA. Our studies highlight the interplay between the DNA binding and photophysical properties necessary for molecules designed to probe the role of DNA as an environmental modulator of electron transfer. They also indicate that intercalation of a donor−linker−acceptor molecule into DNA can give a system that is well-behaved both physically and photochemically. This type of supramolecular assembly can serve as the starting point for the design of systems that give long-lived charge-separated states.

Experimental Section

Synthesis. 5,10,15,20-Tetrakis(4-*N*-methylpyridiniumyl)-21*H*,23*H*-porphyrin, TMPyP(4), was purchased from Mid-Century (Posen, IL) and Porphyrin Products, Inc. (Logan, UT). Other reagents were purchased from Aldrich Chemical, Inc. Anhydrous DMF was used as received from Aldrich. It was sealed and stored under nitrogen. Ferrocenethyl bromide was prepared as described previously.[53] NMR experiments were performed on a Varian VXR-400 instrument operating at 400 MHz. Electrospray mass spectra were taken on a JEOL JMS-XX102/XX102A/E spectrometer operating in positive ion mode.

5-[4-(2-Ferrocenylethyloxy)phenyl]-10,15,20-tris(4-pyridyl)-porphyrin. To a solution of 5-[4-[(ethylcarbonyl)oxy]phenyl]-10,15,20-tris(4-pyridyl)porphyrin[54] (50 mg, 0.074 mmol) in dry DMF (3 mL) under nitrogen was added powdered NaOH (86 mg, 2.15 mmol), and the mixture was stirred for 1 h followed by addition of the ferrocenethyl bromide (36 mg, 0.12 mmol). The mixture was stirred for 5 h at the room temperature, and then the solution was adjusted to pH = 6 with 0.1 M HCl. Water was added and the product was extracted several times with CH_2Cl_2, the combined extracts were dried over Na_2SO_4, the volume of solvent was reduced, and the product was precipitated by addition of petroleum ether, filtered off, and dried. The porphyrin was purified by chromatography (silica gel, CH_2Cl_2/EtOH, 97/3). Evaporation of solvents afforded 26 mg of porphyrin (yield 42%). ^{1}H NMR ($CDCl_3$): 9.05 (m, 6 H, 2,6-pyridine), 8.97 (d, 2 H, J = 4.8 Hz, pyrrole), 8.85 (s, 4 H, pyrrole), 8.82 (d, 2 H, J = 4.4 Hz, pyrrole), 8.17 (d, 6 H, J = 4.4 Hz, 3,5-pyridine), 8.11 (d, 2 H, J = 8.8 Hz, 2,6-phenyl), 7.31 (d, 2 H, J = 8.4 Hz, 3,5-phenyl), 4.20−4.33 (9 H, ferrocene), 4.30 (t, 2 H, J = 6.8 Hz, O−CH_2), 3.05 (t, 2 H, J = 6.8 Hz, CH_2−ferrocene) (see Figure S2 of Supporting Information). MS (FAB) m/z M^+ 845.

5-[4-(2-Ferrocenylethoxy)phenyl]-10,15,20-tris(4-N-methylpyridinumyl)porphyrin, P3Fc. The ferrocenyl porphyrin above was methylated in DMF with a large excess of methyl iodide (100−120 equiv) overnight at room temperature. The methyl iodide and the solvent were removed under vacuum. The residue was taken up in methanol and precipitated with petroleum ether. The resultant product was dried at 60 °C under vacuum. ^{1}H NMR (Me_2SO-d_6, 80 °C): 9.44 (d, 6 H, J = 5.2 Hz, 2,6-pyridine), 9.10 (s, 4 H, pyrrole), 9.04 (d, 2 H, J = 4.8 Hz, pyrrole), 9.02 (d, 2 H, J = 5.2 Hz, pyrrole), 8.95 (d, 6 H, J = 5.6 Hz, 3,5-pyridine), 8.13 (d, 2 H, J = 8.4 Hz, 2,6-phenyl), 7.45 (d, 2 H, J = 8.4 Hz, 3,5-phenyl), 4.71 (s, 9 H, N^+−CH_3), 4.46 (t, 2 H, J = 6.4 Hz, O−CH_2), 4.18−4.36 (9 H, ferrocene), 2.95 (t, 2 H, J = 6.4 Hz, CH_2−ferrocene) (see Figure S2). UV/vis (MeOH) 428, 519, 556, 593, and 651 nm; MS (FAB) m/z 888 (M^+ − 2 H).

DNA Preparation. Calf thymus DNA was obtained from Worthington and prepared as previously described.[55] Buffer solutions employed were N00 = 7.5 mM NaH_2PO_4, 1 mM EDTA, pH 7.0 and N10 = 7.5 mM NaH_2PO_4, 1 mM EDTA, 0.1 M NaCl, pH 7.0. Fresh samples were prepared and used immediately before all spectroscopic measurements. Plastic cuvettes were utilized when possible to reduce adsorption of the porphyrin to the inner surface walls of the optical cells.

UV/vis Absorption and CD Spectra. UV/vis absorption spectra were obtained on either a Perkin-Elmer Lambda-6 or a Shimatzu UV-3101PC UV/vis spectrophotometer. Concentrations of TMPyP(4) and P3Fc stock solutions were determined using their molar absorptivities at the Soret maxima (for TMPyP(4) in MeOH ϵ_{424} = 213 000 M^{-1} cm^{-1} and in buffer ϵ_{422} = 197 000 M^{-1} cm^{-1}; for P3Fc in MeOH ϵ_{428} = 189 000 M^{-1} cm^{-1} and in buffer ϵ_{424} = 180 000 M^{-1} cm^{-1}). DNA titrations were performed in plastic cuvettes where an aliquot of a concentrated DNA solution was added to a 3 mL volume of the porphyrin in buffer solution (typically $\sim 1.2 \times 10^{-5}$ M porphyrin), the solution mixed by repeated inversion, and its absorption measured approximately 10 min afterward. Waiting longer times after DNA addition did not appreciably affect the absorption spectra. Measurements for circular dichroism were performed on a Jasco J-600 spectropolarimeter using quartz cuvettes. Optical densities of the samples were approximately 0.8−1.0 at the Soret maxima. A DNA_{bp}/porphyrin ratio = 25 was used so that the average distance between the porphyrins would be large enough that there would be minimal interaction between them.

Steady-State Fluorescence and Fluorescence Lifetime Measurements. Fluorescence spectra were recorded on an SLM-8000C (SLM Aminco, Inc.) photon counting spectrofluorometer and were corrected for the spectral response of the optical system. To eliminate possible effects of nonisotropic emission from the samples, appropriately oriented (magic angle geometry) polarizers were utilized for all measurements, and a Hoya Y-52 optical filter was used to remove second-order excitation light at 740 nm. Samples were typically 1 mM in concentration with optical densities ∼0.15 at the excitation wavelength. The samples were excited at 369 nm and their relative quantum yields (Φ_{Em}) determined relative to TMPyP-(4) in MeOH. A description of the fluorescence lifetime instrumentation and lifetime fitting procedure has been presented;[56] additional details are available in the Supporting Information.

Results

Synthesis. The syntheses of porphyrins bearing both pyridinium and phenol groups were carried out according to the procedure of Casas et al.[54] Alkylation of the tris(pyridine), mono(phenol)porphyrin with bromoethylferrocene gave the tris-(pyridine), mono(phenyl-OCH_2CH_2ferrocene)porphyrin in 42% yield. Subsequent alkylation of this molecule with methyl iodide in DMF gave the desired water-soluble tris(4-*N*-methylpyridiniumyl), mono(phenyl-OCH_2CH_2ferrocene)porphyrin, P3Fc.

A similar synthetic procedure, starting from the *cis*-bis-(pyridine), bis(phenol)porphyrin, gave the *cis*-bis(4-*N*-methylpyridiniumyl), bis(phenyl-OCH_2CH_2ferrocene)porphyrin (see Supporting Information). This compound was not soluble in water and had only limited solubility in DMSO; it was therefore not examined in these DNA and photophysical studies. The ferrocenyl porphyrins in this study are the first designed to be water-soluble. However, a number of groups have synthesized covalently linked porphyrin−ferrocene species,[57−63] including more elaborate triads[64,65] and systems designed to undergo molecular self-assembly.[66−68] Substituted ferrocenes have also been used as axial ligands to the metal center in metalloporphyrins.[69,70]

Absorption Spectra and Salt-Induced Stacking Interactions. The UV/vis absorption spectra of P3Fc in MeOH and aqueous solution (N00 buffer) closely resemble the spectra of the model TMPyP(4). In MeOH, TMPyP(4) has a Soret band at 424 nm and Q-bands at 515, 550, 591, and 658 nm. By comparison, P3Fc in MeOH shows a Soret band centered at 428 nm and Q-bands located at 519, 556, 593, and 651 nm. In N00 buffer, the Soret band of P3Fc moves to higher energy (425 nm), the Q_y-bands move to lower energies (522 and 562 nm), and the Q_x-bands move to higher energies (583 and 644 nm) relative to the spectrum in MeOH. Similar differences between spectra in water and methanol for 4-*N*-methylpyridiniumyl porphyrins have been observed previously.[71] The weak 440 nm band (91 M^{-1} cm^{-1})[72] of ferrocene is hidden by overlap of the strongly absorbing Soret band of the porphyrin.

Binding of P3Fc to DNA. Binding of P3Fc to DNA results in a 10 nm red shift of the porphyrin Soret maximum, with a hypochromicity (*H*%) of approximately 40% (N00 buffer, Figure S3). Under the same experimental conditions, the Soret maximum of TMPyP(4) shifts 15 nm to the red and decreases by 50%, in agreement with previously reported values for this porphyrin.[73−76] The induced CD spectra for both porphyrins in the presence of DNA as a function of salt concentration are shown in Figure 2. At low salt (N00 buffer) the induced CD

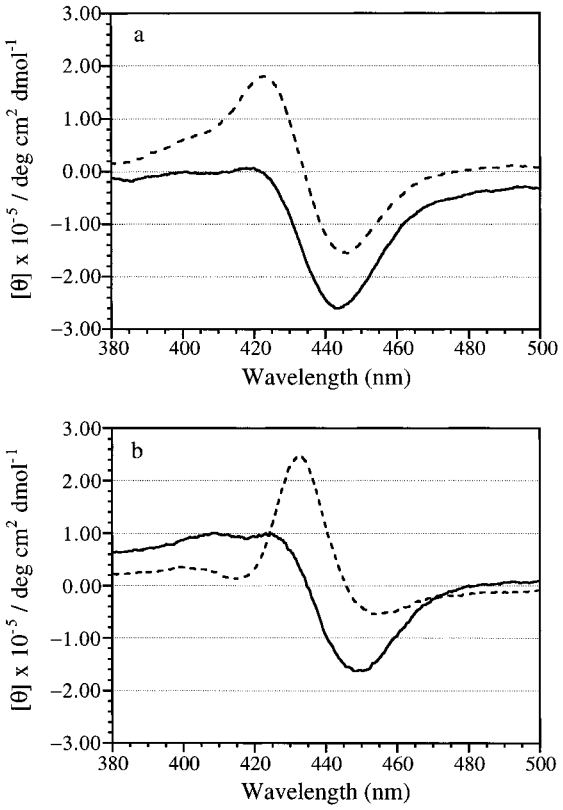

Figure 2. Circular dichroism spectra of (a) TMPyP(4) (8.6×10^{-6} M) and (b) P3Fc (1.0×10^{-5} M) with DNA in N00 pH 7.0 buffer at 25 °C (solid line) and after addition of 100 mM NaCl (dashed line).

spectrum of TMPyP(4) (Figure 2a) in DNA shows a single negative band centered at 442 nm. With addition of 100 mM NaCl, a positive band grows in at 425 nm while the magnitude of the negative band decreases. The induced CD spectrum of P3Fc (Figure 2b) exhibits a negative band at ∼450 nm and a broad positive component centered at ∼423 nm at low salt (N00 buffer). Addition of 100 mM NaCl to the DNA complex causes a significant reduction in the magnitude of the negative component and an increase and red shift of the positive component. Small changes continue if the solution is left over time.

Static Fluorescence in the Absence of DNA. Normalized steady-state fluorescence spectra for TMPyP(4) and P3Fc are displayed in, respectively, Figure 3, a and b, in methanol, N00 buffer, and N00 buffer with DNA. The emission spectrum for TMPyP(4) in MeOH (Figure 3a) contains characteristic peaks in the 660 nm [Q(0,0)-band] and 720 nm [(Q(0,1)-band] regions. This spectrum closely resembles spectra reported in the literature which have also been corrected for instrument response.[71] In N00 buffer, the emission spectrum is broadened and the energy separation of the two bands decreases, producing unresolved vibrational structure. The emission spectrum for P3Fc (Figure 3b) in MeOH also shows well-resolved Q-bands in the 660 and 720 nm regions. As observed for TMPyP(4), the spectrum is broadened, and the energy separation of the two bands decreases in buffer.

Changes in solvent result in changes in the emission intensity as well as the vibrational structure. To quantitate emission intensity changes, emission quantum yields were determined for all compounds in this study relative to the emission intensity of TMPyP(4) in argon-deaerated MeOH, Φ_{Em} (Table 1). Reported values for the absolute emission quantum yields of TMPyP(4) in aqueous solutions include 0.011 (H_2O, pH 5.0),[49]

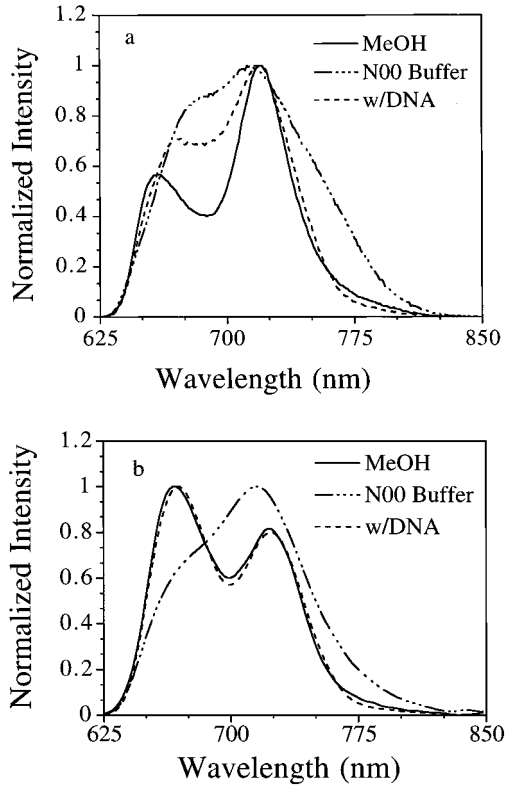

Figure 3. Normalized steady-state emission spectra of (a) TMPyP(4) and (b) P3Fc in N00 pH 7.0 buffer, MeOH and with DNA. Samples were excited at 369 nm and were typically 9×10^{-6} M in porphyrin concentration. Shapes of the bands in the spectra were the same under degassed and air-saturated conditions.

0.047 (H_2O),[50] and 0.024 (10 mM phosphate buffer, pH 7.0).[51] In buffer, TMPyP(4) shows a decrease in emission intensity compared to its intensity in MeOH. In N00 buffer without EDTA the Φ_{em} is 0.70, while in N00 buffer with EDTA the Φ_{Em} is 0.30. The lower Φ_{Em} of TMPyP(4) in the presence of EDTA is presumably due to reductive quenching of the excited state of the porphyrin by the EDTA itself, as observed for other diamagnetic porphyrins.[77,78]

The intensity of the fluorescence from P3Fc in either MeOH or buffer is dramatically reduced compared to that of TMPyP-(4). The Φ_{Em} values for P3Fc in MeOH and N00 buffer are respectively 0.0098 and 0.0076 (Table 1). These numbers are upper limits for Φ_{em} of P3Fc; fluorescence decay data (see below) indicate that there is a small amount ($\leq$1%) of an impurity which is presumably a porphyrin without an attached ferrocene. The low relative quantum yields for P3Fc indicate that the intensity of fluorescence from P3Fc in either MeOH or buffer is <2% of the fluorescence intensity measured for TMPyP(4) under the same conditions. This substantial loss of fluorescence in P3Fc compared to TMPyP(4) is presumably due to reductive quenching of the porphyrin excited singlet state through intramolecular electron transfer from the appended ferrocene donor.

Static Fluorescence in the Presence of DNA. The addition of DNA to buffer solutions of TMPyP(4) and P3Fc results in the appearance of two nearly resolved bands in the steady-state emission spectra for both porphyrins that closely resemble their spectra in MeOH (Figure 3). The fluorescence bands observed for TMPyP(4) in DNA show resolution that is intermediate between that observed in MeOH and that in buffer for this complex. The Φ_{Em} for TMPyP(4) in the presence of DNA is 0.52 in N00 buffer in both the presence and the absence of EDTA. This is lower than that measured without EDTA (0.7) and higher than that measured with EDTA (0.3), indicating that DNA partially protects the TMPyP(4) from quenching by EDTA. Similarly for P3Fc, the Φ_{Em} in DNA (0.011, N00 buffer with EDTA) is slightly higher than its quantum yield in N00 buffer alone (0.0076) (Table 1). However, when compared to the Φ_{Em} of TMPyP(4) in DNA, the fluorescence quantum yield from P3Fc in DNA is still $\geq$98% lower than the fluorescence yield from TMPyP(4).

Fluorescence Decays. Emission decays were obtained for P3Fc and TMPyP(4) in argon-deaerated MeOH and N00 buffer (Table 1). Representative emission decay traces for TMPyP-(4) and P3Fc in MeOH are displayed in Figure 4. In general, the emission decays of TMPyP(4) can be satisfactorily fit by either bi- or triexponential kinetic traces. However, in all cases the reduced chi-squared value (χ_r^2) is better (1.5−5 times) for

TABLE 1: Emission Lifetimes and Relative Emission Quantum Yields (Φ_{Em}) of TMPyP(4) and P3Fc[a]

compound	solvent	DNA_{bp}/porph	(α_1)	τ_1, ns	[area%][b]	(α_2)	τ_2, ns	[area%]	(α_3)	τ_3, ns	[area%]	$\langle\tau\rangle$,[c] ns	χ_r^2 [d]	Φ_{Em}[e]
TMPyP(4)	MeOH	0	(0.23)	1.65	[5%]	(0.77)	10.0	[95%]				8.1	1.3	1.0
			(0.30)	0.51	[2%]	(0.12)	3.44	[6%]	(0.58)	10.3	[91%]	6.6	0.46	
	N00[f]	0	(0.29)	0.31	[3%]	(0.25)	1.64	[16%]	(0.46)	4.49	[81%]	2.6	2.9	0.30
														0.70[g]
	N00:DNA	25	(0.32)	0.74	[4%]	(0.28)	3.56	[18%]	(0.40)	10.9	[78%]	5.5	0.7	0.52
														0.52[g]
	N10:DNA	25	(0.39)	0.28	[2%]	(0.20)	2.83	[12%]	(0.41)	10.5	[86%]	5.0	1.5	
P3Fc	MeOH	0	(0.99)	0.10	[58%]	(0.01)	7.35	[42%]				≤0.11[c]	10[h]	0.0098
	N00	0	(0.99)	0.11	[67%]	(0.01)	3.49	[33%]				≤0.11	3.6[i]	0.0076
	N00:DNA	25	(0.99)	0.14	[56%]	(0.01)	8.78	[44%]				≤0.14	3.7	0.011
			(0.67)	0.11	[31%]	(0.32)	0.19	[25%]	(0.01)	8.78	[44%]	≤0.14	3.0	
	N10:DNA	25	(0.67)	0.10	[28%]	(0.31)	0.24	[28%]	(0.02)	4.81	[43%]	≤0.14	11[j]	

[a] All emission decays obtained on freshly prepared samples placed in quartz cuvettes, bubbled with argon gas for 30 min, and sealed with a Teflon stopper just prior to measurement. Samples were typically $\sim 9 \times 10^{-6}$ M in concentration and were excited at 355 nm with emission monitored at 658 nm. DNA used for these studies was calf thymus DNA. [b] Symbols represent: fractional relative emission amplitudes, (α_i); lifetime in nanoseconds; τ_i; percent relative emission area, [area%] for each decay component. [c] Average lifetimes were calculated according to $\langle\tau\rangle = \sum_i(\alpha_i\tau_i)$ where i is the ith component for the decays. Calculations of the average lifetimes for P3Fc did not include the long-lived emissive component that had an amplitude of 0.01 or 0.02. [d] Reduced chi-squared statistic (χ_r^2). [e] All steady-state emission quantum yields were determined relative to the emission intensity of TMPyP(4) in argon-deareated MeOH. Emission quantum yields for TMPyP(4) were obtained on argon-deareated solutions, while the quantum yields for P3Fc were measured on air saturated solutions (the presence of oxygen would not effect the already short lifetimes of P3Fc). Samples were typically 2.0×10^{-5} M in concentration and were excited at 369 nm. [f] N00 Buffer is 7.5 mM NaH_2PO_4/1 mM EDTA pH 7.0. N10 buffer is N00 buffer with 0.1 M NaCl added. [g] Relative quantum yield for TMPyP(4) in argon-deareated N00 buffer without EDTA. [h] For a triple-exponential fit the χ_r^2 was slightly improved at 7.3; however, the average lifetime remained the same. [i] A triple-exponential fit resulted in a χ_r^2 of 3.3 and $\langle\tau\rangle = 0.17$ ns. [j] The biexpoential fit gave a χ_r^2 of 19.

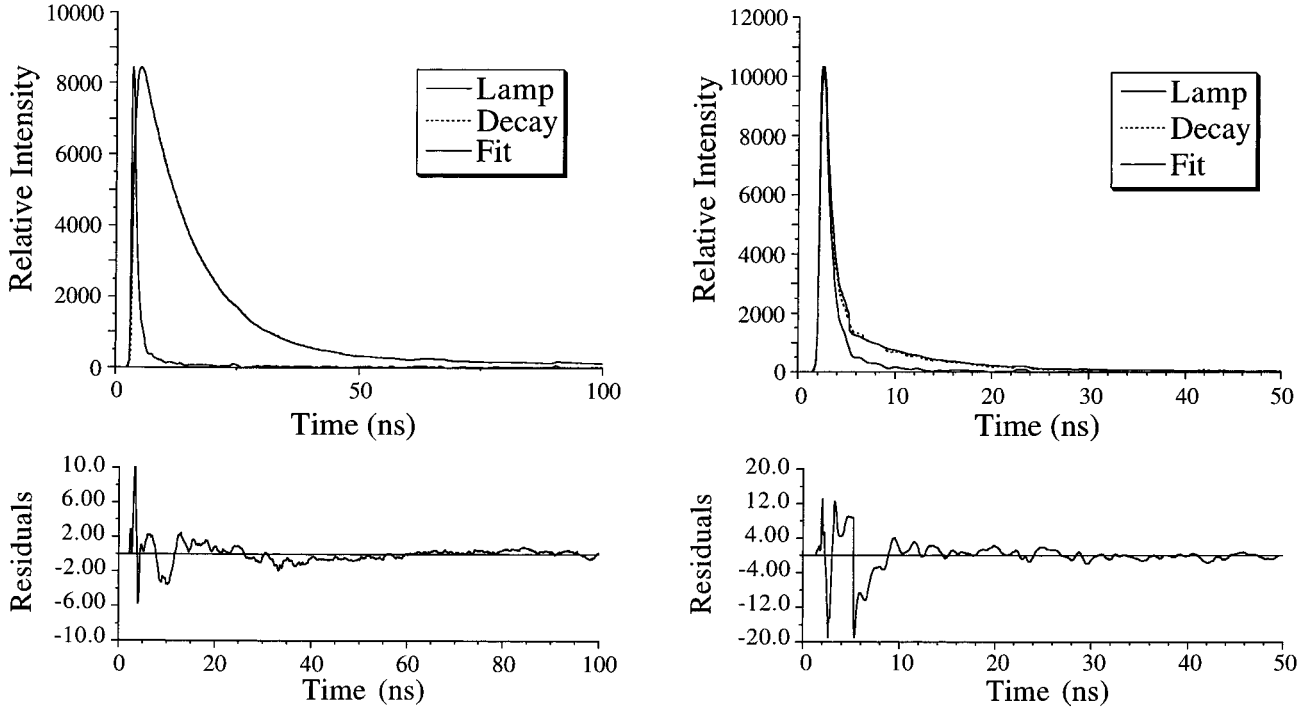

Figure 4. Emission decay kinetics plots for TMPyP(4) (left) and P3Fc (right) in argon-deaerated MeOH. In the top portions of the figure are shown plots of the experimental emission decay monitored at 658 nm (decay), the 355 nm excitation pulse instrument response (lamp), and an iterative reconvolution fit to the biexponential equation, $\alpha_1 \exp(-t/\tau_1) + \alpha_2 \exp(-t/\tau_2) + \alpha_3$, versus time. The bottom portions of the figure show the difference between the calculated fit and the experimental data divided by the noise of the detection system versus time.

the triexponential fits. Both types of fits are given for TMPyP-(4) in Table 1. The biexponential fit to the decay of TMPyP-(4) in MeOH results in lifetimes of 1.65 and 10.0 ns; the triexponential fit gives lifetimes of 0.51, 3.44, and 10.3 ns. The χ_r^2 factor is improved ~3-fold for the triexponential fit. In N00 buffer solution, the emission decay for TMPyP(4) is best fit to a triexponential function with lifetimes of 0.31, 1.64, and 4.49 ns. Compared to the triexponential fit of TMPyP(4) in MeOH, the three lifetime components in buffer are all reduced in length (Table 1), with the largest decrease seen in the longest component (τ_3). The relative amplitude of τ_3 ($\alpha_3 = 0.46$) in buffer is also slightly lower than its amplitude in MeOH ($\alpha_3 = 0.58$). However, fit-to-fit variations of 10−20% in relative emission amplitude are common for multiexponential decays.[79]

The average emission lifetimes for P3Fc are significantly reduced in length compared to those for the model TMPyP(4). The emission decay of P3Fc in MeOH shows biexponential kinetics, resulting in lifetimes of 0.10 and 7.35 ns. The relative amplitude ($\alpha_1 = 0.99$) of the short-lived component indicates that 99% of the sample fluoresces with a lifetime of ca. 100 ps. This very short lifetime probably reflects the temporal resolution of the detection system, which we take as 100−150 ps.[56] The several nanosecond-lived emission components in all samples of P3Fc in Table 1 are likely due to a small amount (≤1%) of an impurity which is a porphyrin without an attached ferrocene. The emission lifetime of such a porphyrin (with three 4-*N*-methylpyridiniumyl groups and one phenolic group) is likely to have a longest emission component in the 5−10 ns range. Nanosecond-lived components in the emission decays of P3Fc were therefore neglected in the calculation of the average lifetimes for this complex (Table 1). In N00 buffer P3Fc can also be fit to a biexponential decay with lifetimes of 0.11 and 3.49 ns. As in MeOH, the short-lived species (0.11 ns) has a relative emission amplitude of 99%, indicating highly efficient quenching; this is in agreement with the very low emission quantum yield data in this solvent.

Fluorescence Decays in DNA. Emission decays for TMPyP-(4) and P3Fc were measured in the presence of DNA in two buffer solutions. The emission decays for TMPyP(4) with DNA are better described by tri- than biexponential fits. In the lower salt N00 buffer, the triexponential fit results in lifetimes of 0.74 ns (τ_1), 3.56 ns (τ_2), and 10.9 ns (τ_3). Similar, although slightly reduced, lifetimes for τ_1 and τ_2 with DNA are seen in N10 buffer (N00 with 0.1 M NaCl). The longest emission lifetime (τ_3, 10−11 ns), which is observed for TMPyP(4) with DNA in both buffers, has an amplitude of 40% and is the same length as that for TMPyP(4) in MeOH. The rank ordering of emission lifetimes (for either two- or three-lifetime fits) agrees with that for the relative emission quantum yields. For example (using results from three-lifetime fits), the corresponding average lifetimes and relative quantum yields for TMPyP(4) in the series MeOH, DNA in N00, and N00 itself are 6.6, 5.5, and 2.6 ns (lifetimes) versus 1.0, 0.52, and 0.30 (yields).

The decay of P3Fc in the presence of DNA in N00 buffer is fit equally well with either two- or three-exponential functions; simplicity favors choosing the two-lifetime fit. Thus, emission quenching within P3Fc is not detectably different whether it is in MeOH, N00 buffer or in the presence of DNA in N00 buffer. In all cases 99% of the fluorescence decays in 100−150 ps. For P3Fc dissolved in N10 buffer (0.1 M NaCl), a three-lifetime fit to the emission decay data is nearly twice as good as a two-lifetime fit, with χ_r^2 values of 11 and 17, respectively. The χ_r^2 factors in both cases are larger than usual, and it is therefore difficult to be sure that increasing the salt concentration by going from N00 to N10 has caused a shift to a more complicated decay pattern. A more complicated pattern at higher salt concentrations would be consistent with an increased number of binding geometries, as indicated by the CD spectrum (Figure 2b). To the extent the triexponential fit is accurate, increasing salt adds a second ca. 240 ps emission decay process to the above-described 100−150 ps decay seen in the three other cases in Table 1.

A point to consider concerning the emission decay for P3Fc is that the decay of the short-lived emission observed for this complex may be even shorter than 100 ps. However, 100−110 ps decays are seen in MeOH and in N00, while somewhat lengthened decays are seen in buffer with DNA. The quantum yield reduction on going from TMPyP(4) to P3Fc in MeOH suggests that the average lifetime of ca. 7 ns for TMPyP(4) could be as low as 40 ps (58% × 0.0098 × 7 ns) for P3Fc, if the two complexes have similar radiative rates. Thus, it is likely that the reported short emission lifetimes for P3Fc are within a factor of 3 of their correct values.

Discussion

The goal of this work was to probe the effect of DNA scaffolding on electron transfer in a donor−linker−acceptor complex. P3Fc was designed for its favorable intercalation, spectroscopic, and electron-transfer characteristics. Below we discuss first the photophysics of P3Fc itself, then the binding of P3Fc to DNA, and finally the electron transfer in P3Fc bound to DNA.

Electron Transfer in P3Fc. P3Fc possesses significantly reduced relative emission quantum yields and average lifetimes in both MeOH and buffer compared to TMPyP(4) as seen in Table 1. In fact, the emission yield for P3Fc in both MeOH and N00 buffer without EDTA is only 1% of that of TMPyP(4) in MeOH and N00 without EDTA, respectively, indicating a 99% reduction in fluorescence for the P3Fc complex versus TMPyP(4). Similar, although less efficient, fluorescence quenching in methylene chloride has been observed for a porphyrin−ferrocene−quinone compound[65] as well as for a series of neutral porphyrin−ferrocene complexes studied by Wrighton and co-workers.[52] As in the latter study, we ascribe fluorescence quenching in P3Fc to electron transfer rather than energy transfer.

The overall free energy change for photoinduced electron transfer in P3Fc can be determined from the redox potentials of the reactants and the energy of the porphyrin's S_1 excited state according to[80]

$$\Delta G^\circ = e[E_{1/2}(D^{\bullet+}/D) - E_{1/2}(A/A^{\bullet-})] - \Delta E(0,0) + w(r) \quad (1)$$

where e is the charge on the electron, $E_{1/2}$ is a half-wave reduction for potential either for the donor ($D^{\bullet+}$/D) or acceptor ($A/A^{\bullet-}$) couples in volts, $\Delta E(0,0)$ is the relevant excited-state energy, and $w(r)$ is a Coulombic interaction term between the oxidized donor and reduced acceptor which represents energy stored in the ionic products due to separating them a distance (r) relative to each other; $w(\infty) = 0$.[81,82] Generally in very polar media the Coulombic term is less than ca. 0.1 eV and will be neglected here. For P3Fc in a polar solvent the thermodynamic driving force for photoinduced intramolecular electron transfer is −0.66 eV based on eq 1 and the following values: $E_{1/2}(P3^{3+}/P3^{2+}) = -0.73$ eV (vs SCE in DMF),[83] where P3 is tris(4-*N*-methylpyridiniumyl) (monophenyl)porphyrin; $E_{1/2}$ (Fc^+/Fc) = 0.5 eV (vs SCE in CH_2Cl_2);[52,60] and $\Delta E(0,0) = 1.89$ eV for the S_1 state of P3Fc. The ΔG° estimate of −0.66 eV for photoinduced electron transfer within P3Fc strongly suggests that its strikingly reduced average emission lifetime and yield versus TMPyP(4) are due to electron transfer from ferrocene to the photoexcited porphyrin.

Although the free energy for electron transfer from ferrocene to the S_1 state of the porphyrin is P3Fc is strongly exothermic, two other singlet state quenching possibilities should be considered. The first of these is enhanced intersystem crossing from the porphyrin's S_1 state to its lowest triplet state (T_1) as a result of appending the ferrocene. Wrighton and co-workers examined this question in three porphyrin−linker−ferrocene complexes.[52] In the Wrighton studies, the porphyrin was the hydrophobic 5,15-bis(4-tolyl)-2,3,7,8,12,13,17,18-octamethylporphyrin (OMP), and the linkers were C−C chains (CH_2-CH_2, *trans*-CH═CH, and *cis*-CH═CH).[52] For both the CH_2CH_2 and vinyl cases, transient absorbance measurements of the triplet yield indicated that little or no enhancement of intersystem crossing occurred relative to that found for OMP itself. A second possible singlet state quenching channel is energy transfer from the porphyrin's S_1 state to ferrocene. However, such energy transfer would be strongly endothermic because the singlet excited state of ferrocene (2.46 eV)[72] is 0.57 eV above that of the S_1 state of the porphyrin (1.89 eV). Thus, neither enhanced intersystem crossing within the porphyrin nor energy transfer from the porphyrin to ferrocene is a reasonable process to explain the very fast (≤0.11 ns) singlet excited state quenching observed in P3Fc. On the other hand, electron-transfer quenching is very strongly favored on thermodynamic grounds. Note that electron transfer in P3Fc ($\Delta G^\circ = -0.66$ eV) is substantially more exothermic than in the three OMP−linker−Fc complexes ($\Delta G^\circ = -0.11$ to −0.07 eV), in which fluorescence quenching was also attributed to electron transfer.

Rates of Electron Transfer in Ferrocenyl Porphyrins. Estimates of the average rate of forward intramolecular electron transfer (k_{ET}) from the appended ferrocene to the photoexcited cationic porphyrin and in P3Fc can be made based on the average emission lifetimes of P3Fc ($\langle\tau\rangle$) and the model compound TMPyP(4) ($\langle\tau_0\rangle$) according to eq 2:

$$k_{ET} = 1/\langle\tau\rangle - 1/\langle\tau_0\rangle \quad (2)$$

Using eq 2, the average lifetimes for TMPyP(4) from the triexponential fits, and the subnanosecond lifetimes for P3Fc in Table 1, the average rate of intramolecular electron transfer from the ferrocene to the porphyrin in P3Fc is calculated to be $\geq 1 \times 10^{10}$ s^{-1} in MeOH, 9×10^9 s^{-1} in N00 buffer without DNA, and 7×10^9 s^{-1} in N00 buffer with DNA. All three of these electron-transfer rates are considerably faster than the rates determined for the three OMP−linker−Fc complexes in Wrighton's study. Specifically, k_{ET} for P3Fc is at least 1500 times faster than the rate measured for OMP−CH_2CH_2−Fc ($k_{ET} = 4.8 \times 10^6$ s^{-1}), 700 times faster than the rate for OMP-*trans*-CH═CH−Fc ($k_{ET} = 1.0 \times 10^7$ s^{-1}), and 40 times faster than the rate for OMP-*cis*-CH═CH−Fc ($k_{ET} = 1.8 \times 10^8$ s^{-1}).[52] Further quantitative comparison of the observed electron-transfer rates for P3Fc and the OMP−linker−Fc complexes would require explicit consideration not only of their substantial driving force differences but also of their solvent differences (CH_2Cl_2 for the OMP complexes vs water for P3Fc). This latter analysis quickly becomes speculative due to uncertainties in the solvent reorganization energies[43,44] and will not be pursued here.

P3Fc Binding to DNA. Three relatively well-defined modes have been described for the binding of cationic porphyrins to DNA: intercalation, outside binding, and outside binding with self-stacking of the porphyrin.[75,76,84] Intercalation is indicated by a red shift in the position and a substantial reduction in the intensity of the Soret band of the bound porphyrin intercalator, by an increase in the relative viscosity of closed circular DNA, and by a single negative induced CD band in the Soret region. Porphyrins that bind outside the DNA duplex but without self-stacking (e.g., metalloporphyrins with axial ligands) show smaller changes in the shift and intensity of the Soret band and a single positive induced CD band in the Soret region.

Porphyrins with a tendency to self-stack in solution have additional modes of interaction that involve outside binding of various stacked forms of the porphyrin with DNA. Such binding is indicated by strong induced CD signals (3−100-fold larger than bands from intercalated complexes) containing both positive and negative components.[85−91] Because the free energies of these binding modes can be similar, and because the binding mode depends on both the ionic strength and pH of the solution as well as the sequence of the DNA, a given porphyrin may adopt more than one binding mode depending on these conditions.

Studies from a number of groups have shown that the parent TMPyP(4) is an intercalator in calf thymus DNA.[75,76,84] The binding constant with CT DNA is 1×10^7 M^{-1} (based on competition with ethidium, 0.1 M Tris-HCl buffer, pH 7.4, 0.1 M NaCl, 25 °C).[45] Related studies with $[poly(dA\text{-}dT)]_2$ and $[poly(dG\text{-}dC)]_2$ give binding constants of 4.0×10^6 M^{-1} for both homopolymers at 0.115 M Na^+.[76] These values are the same although TMPyP(4) interacts with $[poly(dA\text{-}dT)]_2$ as an outside binder and $[poly(dG\text{-}dC)]_2$ as an intercalator.[75,76,84] As observed for many cationic DNA binding molecules,[92] the equilibrium constant (K) increases as the salt concentration of the aqueous solution decreases.[76] Plots of log K vs log $[Na^+]$ for TMPyP(4) have a slope of −2.7,[76] leading one to predict a binding constant $>10^9$ M^{-1} in N00 buffer.

Studies of monophenyl-tris(4-*N*-methylpyridiniumyl) porphyrins indicate that this ring system also is an intercalator in DNA. In a detailed study, Sari et al. have shown that tris(4-*N*-methylpyridiniumyl)(monophenyl)porphyrin, P3, binds via intercalation based on the bathochromic shift and intensity decrease of the Soret peak, energy transfer between CT DNA and the porphyrin, and DNA lengthening observed by viscometry.[45] P3 had an apparent binding constant of 3×10^6 M^{-1} at $\mu = 0.2$ M, only about 3-fold lower than that of TMPyP(4) under the same conditions (1×10^7 M^{-1}).[45] Munson and Fiel have investigated the binding of P3 to DNA by measuring the relaxation of porphyrin-induced positively supercoiled DNA using eukaryotic topoisomerase I.[48] They find that both TMPyP(4) and P3 bind to DNA by intercalation and that nearly equivalent concentrations of these two porphyrins result in similar degrees of unwinding. In related work, Bütje and Nakamoto have shown that Ni(II)P3 has a resonance Raman spectrum very similar to that of Ni(II)TMPyP(4), indicating that it is an intercalator also.[46] Resonance Raman studies of copper 4-*N*-methylpyridiniumyl derivatives with $[poly(dG\text{-}dC)]_2$ also indicate that the Cu(II)P3 is an intercalator, though not as strong an intercalator as Cu(II)TMPyP(4).[47] The subject of the current study, P3Fc, has three 4-*N*-methylpyridiniumyl and one uncharged side chains and thus would be expected to intercalate into DNA. Large side chains on pyridiniumyl porphyrins are not an intrinsic barrier to intercalation; TMPyP(4) homologs with propyl,[93] butyl,[73] hydroxyethyl,[93,94] and $CH_2CH_2CH_2N^+Me_3$ side chains[95] are all known to intercalate in DNA.[96]

Circular dichroism spectroscopy is a useful tool in probing the binding of small molecules to DNA. As outlined above, the induced CD spectra of DNA-bound cationic porphyrins show distinct signatures that correlate with the binding mode. Intercalation is indicated by a negative band, binding to the exterior of the DNA without self-stacking is indicated by a positive band, and binding to the exterior of the DNA with self-stacking is indicated by a conservative CD signal (both positive and negative bands) which has a larger intensity (3−100-fold more intense) than intercalated CD bands. Figure 2a shows the induced CD spectrum of TMPyP(4) in DNA at low (N00 buffer) and moderate (N00 buffer with 0.1 M NaCl) ionic strength. Very similar CD spectra for TMPyP(4) have been observed previously.[97] At low ionic strength, the CD spectrum is negative, the classic signature of an intercalator. When the ionic strength is increased with the addition of 0.1 M NaCl, the negative band decreases in intensity and a positive band grows in at higher energies.[97] This is consistent with a geometry that is largely or exclusively intercalative at low ionic strengths with conversion to a mixture of intercalated and externally bound porphyrin as the ionic strength is increased.

The CD spectrum of P3Fc in DNA shows a number of characteristics similar to TMPyP(4). At low ionic strength, the signal is largely negative. There is some diffuse positive signal to the blue which may represent externally bound P3Fc. When the ionic strength of the P3Fc/DNA solution was raised by the addition of 0.1 M NaCl, the negative band decreased and the positive band increased in magnitude. These changes are qualitatively similar to those observed for TMPyP(4), although the shapes of the CD bands indicate that adding 0.1 M NaCl has a larger effect on P3Fc than on TMPyP(4). The strength of the CD signal is approximately the same at both ionic strengths. This indicates that the porphyrin is still bound to the DNA at the higher ionic strength; had it dissociated from the DNA, the signal strength would have decreased because the porphyrin is achiral and has no CD signal in the absence of close association with the DNA.[97] The similarity of the signal strengths in the two buffers also indicates that the externally bound P3Fc does not self-stack significantly. Had it adopted a self-stacking geometry on the exterior of the DNA, the CD signal would have increased in intensity. The greater sensitivity in DNA of P3Fc compared to TMPyP(4) with respect to changes in the ionic strength parallels studies on these porphyrins in solution without DNA. In the absence of DNA, P3Fc undergoes self-stacking as the ionic strength of a solution increases[98] while TMPyP(4) is relatively insensitive to salt up to NaCl concentrations of 2.0 M.[86,99] For the purposes of the photoinduced electron-transfer experiments, these CD data indicate that P3Fc is largely intercalated in DNA in N00 buffer.

DNA Intercalation Effects on the Spectra and Lifetimes of TMPyP(4). The emission characteristics of TMPyP(4) with DNA in aqueous solution are more similar to their characteristics in the lower dielectric solvent MeOH than to their characteristics in water. Intercalation of TMPyP(4) into DNA results in the appearance of vibronic structure in the emission spectrum and increased lengths of the emission decays, indicating that the DNA protects the porphyrin in part from the surrounding aqueous buffer solution. The three emission components for TMPyP(4) in N00 buffer with DNA bear a striking similarity to the three lifetimes found in MeOH: 0.74, 3.56, and 10.9 ns (N00 with DNA) versus 0.51, 3.44, and 10.3 (MeOH). Each lifetime component seen for TMPyP(4) in N00 aqueous buffer is lengthened slightly more than 2-fold in N00 buffer with DNA. Lui and Koningstein have also found that binding TMPyP(4) to DNA changed the decays, from <4.5 and 5.0 ns in buffer to 1.7 and 10 ns when bound to DNA.[100] We also observe that as the ionic strength of the solution with DNA is increased by the addition of 0.1 M NaCl, the shortest lifetime component decreases the most (0.74−0.28 ns) and achieves its value in N00 buffer without DNA (0.31 ns). Assignment of specific emission decays to specific binding geometries of TMPyP(4) on DNA is probably unwarranted. TMPyP(4) itself has two or three emission decays even in the absence of DNA, as observed in a number of laboratories[49,51,71,99,101−105] (see Supporting Information for a more detailed discussion). Given the intrinsic

multiexponential decay of TMPyP(4), it is likely that the fit to two or three exponentials in the TMPyP(4)/DNA system represents a mathematical description of an ensemble of decays, rather than two or three distinct porphyrin/DNA binding geometries.[100]

DNA Intercalation Effects on k_{ET} for P3Fc. Intercalating part of a donor−linker−acceptor complex into a DNA duplex allows study of how the DNA scaffolding modulates electron transfer. The data in Table 1 for biexponential fits show that intercalation of P3Fc into DNA results in lengthening of both emission decays, with the shorter decay increasing from 0.11 to 0.14 ns and the longer from 3.49 to 8.78 ns. Both in solution and in DNA, however, essentially all of the amplitude is due to the shorter component ($\alpha_1 = 99\%$, with the long-lived component likely arising from an impurity porphyrin lacking ferrocene). These observations are consistent with very fast electron transfer from the ferrocene to the S_1 state of the porphyrin which is affected only minimally by DNA binding. The short linker chain in P3Fc, OCH_2CH_2, is expected to result in electron transfer that proceeds mainly through the linker's bonds. A longer linker might have afforded larger changes upon binding to the scaffold, as observed previously in a $Ru(bpy)_3^{2+}$−linker−viologen system with cyclodextrin as a scaffold.[106] However, longer methylene-based linkers will make the molecule more hydrophobic.

In general, more hydrophobic porphyrins self-stack more readily in aqueous solution.[98] The correlation between the tendency of a porphyrin to self-stack in solution upon the addition of NaCl and its tendency to bind to the exterior of duplex DNA in a self-stacked form has been noted in a number of instances.[48,85,88−91,99,107−109] P3Fc undergoes salt-induced self-stacking in aqueous solution;[98] the butyl homologue of TMPyP(4) does as well.[98] The P3Fc (this work) and butyl homologue of TMPyP(4)[73] show very similar CD signatures when bound to CT DNA, with both positive and negative features. Although the magnitude of the CD signal does not indicate significant self-stacking for P3Fc or the butyl homolog, both of these are sensitive to salt in a way that is intermediate between intercalators such as TMPyP(4) and molecules which bind to DNA with self-stacking. Homologs of P3Fc with longer hydrophobic side/linker chains are likely, therefore, to stack on the exterior of the DNA rather than intercalate between the DNA base pairs. This issue highlights the interplay between the DNA binding and the photophysical properties necessary for molecules designed to probe the role of DNA as an electron-transfer modulator.

DNA Scaffolding Effects on Electron Transfer. Intercalation of part of a donor−linker−acceptor molecule into scaffolding results in a number of changes that may alter the rate of electron transfer between the donor and acceptor. One effect of DNA scaffolding may be to change the redox potentials of the donor and acceptor. An intercalated acceptor might be expected to be somewhat more difficult to reduce, based on the transfer from aqueous solution to a more hydrophobic environment. Studies by Anderson and co-workers have shown that intercalation of nitroacridines into DNA lowers their reduction potential by approximately 50 mV.[37] Kelley et al. have observed a similar decrease for the reduction potential of methylene blue intercalated in DNA.[38] A groove-bound donor should be easier to oxidize in the groove than in solution because it resides near negatively charged phosphate groups when bound to DNA. Experimental reduction potentials for groove-bound $Os(bpy)_3^{3+}$ include shifts to less positive redox potentials of 14 mV (75 mM Na^+) and 35 mV (15 mM Na^+).[40,41] The dependence of the reduction potential on ionic strength reflects the ionic strength dependence of the binding constants of the groove bound redox couple. Similar changes have been measured for $Ru(bpy)_3^{3+}$, $Fe(bpy)_3^{3+}$, and $Co(bpy)_3^{3+}$.[39,40,42] To a first approximation, the shifts in the reduction potentials for a groove-bound donor ($D^{\bullet+}$/D) and intercalated acceptor (A/$A^{\bullet-}$) are of the same direction and magnitude. Thus, not only are the redox potential changes due to intercalating P3Fc into DNA likely to be modest, but more difficult reduction of the intercalated porphyrin is likely to be offset by easier oxidation of the groove-bound ferrocene.

Intercalation of one portion of a flexible D−L−A molecule into DNA will also bias the set of conformations that the molecule can adopt in that the scaffolding prevents close approach of the donor and acceptor. The electronic coupling for the D−L−A molecule in scaffolding is expected to be through-bond; the coupling when the D−L−A molecule is free in solution can have both through-bond and direct donor−acceptor contact contributions. Thus, the change in the available conformational sets to ones with greater donor−acceptor distances is expected to decrease the rate of electron transfer. Mallouk and co-workers have observed a decrease in the rate of intramolecular electron transfer in their study of the effect of added cyclodextrin (which binds to the linker) on electron transfer in a $Ru(bpy)_3^{2+}$−linker−viologen molecule.[106] This conformation-controlled decrease in electron-transfer rates for D−L−A molecules in scaffolding arises from a decrease in electronic coupling between the donor and acceptor as well as from some increase in the outer-sphere reorganization energy of the reaction due to increasing the separation between the donor and acceptor. Intercalation of the donor or acceptor may also increase the reorganization energy for electron transfer because the reorganization energy, governed by the dielectric constant of the surrounding medium, is higher in less polar solvents.[23,43,44] Finally, our data for P3Fc showing only a very modest decrease in the rate of electron transfer upon intercalation in DNA (7×10^9 s^{-1} in DNA vs 9×10^9 s^{-1} in N00 buffer) indicate that intercalation of the porphyrin subunit into the π-stack of the DNA has no major effect per se on the rate constant for electron transfer from the ferrocene to the photoexcited porphyrin.

Conclusion

The present study has shown that binding of the tricationic porphyrin−ferrocene complex P3Fc to double-stranded DNA strongly depends on the ionic strength of the solvent. Intercalation is the predominant binding mode for the porphyrin to DNA under low salt conditions (∼10 mM); raising the salt (∼100 mM) shifts the binding to an outside stacking mode. This salt sensitivity is ascribed to the hydrophobic nature of P3Fc, which is also indicated by its propensity to undergo salt-induced stacking in aqueous solution. Fluorescence from the porphyrin is strongly quenched by the appended ferrocene at near unity efficiency. Photoinduced electron transfer is the most likely mechanism responsible for the quenching based on the strong driving force ($\Delta G^\circ = -0.66$ eV) for this reaction. The average rate of photoinduced electron transfer for this complex is $\geq 1 \times 10^{10}$ s^{-1} in MeOH and 9×10^9 s^{-1} in N00 buffer. In the presence of DNA, under conditions where intercalation of the porphyrin is favored and contact between the donor and acceptor is restricted, k_{ET} decreases only modestly to 7×10^9 s^{-1}. Assuming that for this donor−linker−acceptor assembly, in which the ferrocene donor and porphyrin acceptor are separated by a short $-OCH_2CH_2-$ spacer, intercalation of the porphyrin

into DNA does not significantly reduce the electronic coupling between the donor and acceptor, the similarity of the electron-transfer rates in and out of DNA show that changes in redox potentials or reorganization energy either compensate one another or have negligible kinetic consequences.

Supporting Information Available: Synthesis and characterization of 5,10-bis[4-(2-ferrocenylethoxy)phenyl]-15,20-bis-(4-*N*-methylpyridinumyl)porphyrin; NMR spectrum of P3Fc; UV/vis absorption spectrum of P3Fc with DNA; description of the fluorescence lifetime instrumentation and fitting procedure; discussion of the emission decays of TMPyP(4) (7 pages). Ordering information is given on any current masthead page.

Acknowledgment. This work was supported in part by the National Institutes of Health (AI127196 to D.W.D.) and the National Science Foundation (CHE-9709318 to T.L.N.). We thank K. Nafisi, M. Zhao, and H. Halford for technical assistance and Dr. W. D. Wilson for a gift of DNA.

References and Notes

(1) Fox, M. A.; Chanon, M. *Photoinduced Electron Transfer*; Elsevier: Amsterdam, 1988.
(2) Zamareaev, K. I.; Khairutdinov, R. F. *Top. Curr. Chem.* **1992**, *163*, 1−94.
(3) Paddon-Row, M. N. *Acc. Chem. Res.* **1994**, *27*, 18−25.
(4) Kavarnos, G. J. *Fundamentals of Photoinduced Electron Transfer*; VCH: New York, 1993.
(5) Balzani, V. *Tetrahedron* **1992**, *48*, 10443−10514.
(6) Isied, S. S. *Adv. Chem. Ser.* **1997**, *253*, 331−347.
(7) Sutin, N. In *Electron Transfer in Inorganic, Organic and Biological Systems*; Bolton, J. R., McLendon, G., Mataga, N. Eds.; American Chemical Society: Washington, DC, 1991; pp 191−199.
(8) Wasielewski, M. R. *Chem. Rev.* (*Washington, D.C.*) **1992**, *92*, 435−461.
(9) McLendon, G.; Hake, R. *Chem. Rev.* (*Washington, D.C.*) **1992**, *92*, 481−490.
(10) Gust, D.; Moore, T. A.; Moore, A. L. *Acc. Chem. Res.* **1993**, *26*, 198−205.
(11) Nocek, J. M.; Zhou, J. S.; Deforest, S.; Priyadarshy, S.; Beratan, D. N.; Onuchic, J. N.; Hoffman, B. M.; Risser, S. M. *Chem. Rev.* **1997**, *100*, 117678−17682.
(12) Durham, B.; Millett, F. *J. Chem. Educ.* **1997**, *74*, 636−640.
(13) Nicolini, C. *Molecular Bioelectronics*; World Scientific: Singapore, 1996.
(14) Petty, M. C.; Bryce, M. R.; Bloor, D. *An Introduction to Molecular Electronics*; Oxford University Press: New York, 1995.
(15) Sienicki, K. *Molecular Electronics and Molecular Electronic Devices*; CRC Press: Boca Raton, FL, 1993.
(16) Ashwell, G. *Molecular Electronics*; Wiley: New York, 1992.
(17) Kirsch-De Mesmaeker, A.; Lecomte, J. P.; Kelly, J. M. *Top. Curr. Chem.* **1996**, *177*, 25−76.
(18) Carter, P. J.; Ciftan, S. A.; Sistare, M. F.; Thorp, H. H. *J. Chem. Educ.* **1997**, *74*, 641−645.
(19) Netzel, T. L. *J. Chem. Educ.* **1997**, *74*, 646−651.
(20) Symons, M. C. R. *Free Radical Biol. Med.* **1997**, *22*, 1271−1276.
(21) Stemp, E. D. A.; Barton, J. K. *Metal Ions Biol. Syst.* **1996**, *33*, 325−365.
(22) Beratan, D. N.; Priyadarshy, S.; Risser, S. M. *Chem. Biol.* **1997**, *4*, 3−8.
(23) Netzel, T. L. In *Molecular and Supramolecular Photochemistry*; Ramamurthy, V., Schanze, K. S., Eds.; Marcel Dekker: New York, in press.
(24) Barbara, P. F.; Olson, E. J. C. *Adv. Chem. Phys.*, in press.
(25) Tuite, E. In *Molecular and Supramolecular Photochemistry*; Ramamurthy, V., Schanze, K. S., Eds.; Marcel Dekker: New York, in press.
(26) Murphy, C. J.; Arkin, M. R.; Jenkins, Y.; Ghatlia, N. D.; Bossmann, S. H.; Turro, N. J.; Barton, J. K. *Science* **1993**, *262*, 1025−1029.
(27) Meade, T. J.; Kayyem, J. F. *Angew. Chem., Int. Ed. Engl.* **1995**, *34*, 352−354.
(28) Lewis, F. D.; Wu, T.; Zhang, Y.; Letsinger, R. L.; Greenfield, S. R.; Wasielewski, M. R. *Science* **1997**, *277*, 673−676.
(29) Brun, A. M.; Harriman, A. *J. Am. Chem. Soc.* **1994**, *116*, 10383−10393.
(30) Olson, E. J. C.; Hu, D. H.; Hormann, A.; Barbara, P. F. *J. Phys. Chem. B* **1997**, *101*, 299−303.
(31) Kelley, S. O.; Holmlin, R. E.; Stemp, E. D.; Barton, J. K. *J. Am. Chem. Soc.* **1997**, *119*, 9861−9870.
(32) Taubes, G. *Science* **1997**, *275*, 1420−1421.
(33) Netzel, T. L. *J. Biol. Inorg. Chem.*, in press.
(34) Lincoln, P.; Tuite, E.; Nordén, B. *J. Am. Chem. Soc.* **1997**, *119*, 1454−1455.
(35) Schulman, L. S.; Bossmann, S. H.; Turro, N. J. *J. Phys. Chem.* **1995**, *99*, 9283−9292.
(36) Orellana, G.; Kirsch-De Mesmaeker, A.; Barton, J. K.; Turro, N. J. *Photochem. Photobiol.* **1991**, *54*, 499−509.
(37) Anderson, R. F.; Patel, K. B.; Wilson, W. R. *J. Chem. Soc., Faraday Trans.* **1991**, *87*, 3739−3746.
(38) Kelley, S. O.; Barton, J. K.; Jackson, N. M.; Hill, M. G. *Bioconjug. Chem.* **1997**, *8*, 31−37.
(39) Carter, M. T.; Rodríguez, M.; Bard, A. J. *J. Am. Chem. Soc.* **1989**, *111*, 8901−8911.
(40) Rodriguez, M.; Bard, A. J. *Anal. Chem.* **1990**, *62*, 2658−2662.
(41) Welch, T. W.; Thorp, H. H. *J. Phys. Chem.* **1996**, *100*, 13829−13836.
(42) Johnston, D. H.; Thorp, H. H. *J. Phys. Chem.* **1996**, *100*, 13837−13843.
(43) Gosztola, D.; Wang, B.; Wasielewski, M. R. *J. Photochem. Photobiol. A* **1996**, *102*, 71−80.
(44) Zhang, X.; Kozik, M.; Sutin, N.; Winkler, J. R. In *Electron Transfer in Inorganic, Organic and Biological Systems*; Bolton, J. R., McLendon, G., Mataga, N., Eds.; American Chemical Society: Washington, DC, 1991; pp 247−264.
(45) Sari, M. A.; Battioni, J. P.; Dupré, D.; Mansuy, D.; Le Pecq, J. B. *Biochemistry* **1990**, *29*, 4205−4215.
(46) Bütje, K.; Nakamoto, K. *J. Inorg. Biochem.* **1990**, *39*, 75−92.
(47) Strahan, G. D.; Lu, D.; Tsuboi, M.; Nakamoto, K. *J. Phys. Chem.* **1992**, *96*, 6450−6457.
(48) Munson, B. R.; Fiel, R. J. *Nucl. Acids Res.* **1992**, *20*, 1315−1319.
(49) Kalyanasundaram, K.; Neumann-Spallart, M. *J. Phys. Chem.* **1982**, *86*, 5163−5169.
(50) Kalyanasundaram, K. *Inorg. Chem.* **1984**, *23*, 2453−2459.
(51) Ito, A. S.; Azzellini, G. C.; Silva, S. C.; Serra, O.; Szabo, A. G. *Biophys. Chem.* **1992**, *45*, 79−89.
(52) Giasson, R.; Lee, E. J.; Zhao, X.; Wrighton, M. S. *J. Phys. Chem.* **1993**, *97*, 2596−2601.
(53) Shu, C.-F.; Anson, F. C. *J. Phys. Chem.* **1990**, *94*, 8345−8350.
(54) Casas, C.; Saint-Jalmes, B.; Loup, C.; Lacey, C. J.; Meunier, B. *J. Org. Chem.* **1993**, *58*, 2913−2917.
(55) Davidson, M. W.; Griggs, B. G.; Boykin, D. W.; Wilson, W. D. *J. Med. Chem.* **1977**, *20*, 1117−1122.
(56) Netzel, T. L.; Zhao, M.; Nafisi, K.; Headrick, J.; Sigman, M. S.; Eaton, B. E. *J. Am. Chem. Soc.* **1995**, *117*, 9119−9128.
(57) Wollmann, D. G.; Hendrikson, D. N. *Inorg. Chem.* **1977**, *16*, 3079−3089.
(58) Hisatome, M.; Takano, S.; Yamakawa, K. *Tetrahedron Lett.* **1985**, *26*, 2347−2350.
(59) Beer, P. D.; Kurek, S. S. *J. Organomet. Chem.* **1987**, *336*, C17−C21.
(60) Vaijayanthimala, G.; D'Souza, F.; Krishnan, V. *J. Coord. Chem.* **1990**, *21*, 333−342.
(61) Beer, P. D.; Drew, M. G. B.; Jagessar, R. *J. Chem. Soc., Dalton Trans.* **1997**, 881−886.
(62) Beer, P. D.; Drew, M. G. B.; Hesek, D.; Jagessar, R. *J. Chem. Soc., Chem. Commun.* **1995**, 1187−1189.
(63) Burrell, A. K.; Campbell, W.; Officer, D. L. *Tetrahedron Lett.* **1997**, *38*, 1249−1252.
(64) Wagner, R. W.; Johnson, T. E.; Lindsey, J. S. *Tetrahedron* **1997**, *53*, 6755−6790.
(65) Beer, P. D.; Kurek, S. S. *J. Organomet. Chem.* **1989**, *366*, C6−C8.
(66) Tecilla, P.; Dixon, R. P.; Slobodkin, G.; Alavi, D. S.; Waldeck, D. H.; Hamilton, A. D. *J. Am. Chem. Soc.* **1990**, *112*, 9408−9410.
(67) Wagner, R. W.; Brown, P. A.; Johnson, T. E.; Lindsey, J. S. *J. Chem. Soc., Chem. Commun.* **1991**, 1463−1466.
(68) Cesario, M.; Giannotti, C.; Guilhem, J.; Silver, J.; Zakrzewski, J. *J. Chem. Soc., Dalton Trans.* **1997**, 47−53.
(69) Schmidt, E. S.; Calderwood, T. S.; Bruice, T. C. *Inorg. Chem.* **1986**, *25*, 3718−3720.
(70) Zakrzewski, J.; Giannotti, C. *J. Chem. Soc., Chem. Commun.* **1992**, *1992*, 662−663.
(71) Vergeldt, F. J.; Koehorst, R. B. M.; Van Hoek, A.; Schaafsma, T. J. *J. Phys. Chem.* **1995**, *99*, 4397−4405.
(72) Sohn, Y. S.; Hendrickson, D. N.; Gray, H. B. *J. Am. Chem. Soc.* **1971**, *93*, 3603−3612.
(73) Sehlstedt, U.; Kim, S. K.; Carter, P.; Goodisman, J.; Vollano, J. F.; Nordén, B.; Dabrowiak, J. C. *Biochemistry* **1994**, *33*, 417−426.
(74) Gibbs, E. J.; Pasternack, R. F. *Semin. Hematol.* **1989**, *26*, 77−85.
(75) Fiel, R. J. *J. Biomol. Struct. Dyn.* **1989**, *6*, 1259−1273.

(76) Marzilli, L. G. *New J. Chem.* **1990**, *140*, 4090−4200.
(77) Shen, C. Y.; Kostić, N. M. *Inorg. Chem.* **1996**, *35*, 2780−2784.
(78) Karmakar, A.; Chaudhuri, R.; Bera, S. C.; Rohatgi-Mukherjee, K. K. *Indian J. Chem., Sect. A* **1995**, *34*, 83−93.
(79) Vix, A.; Lami, H. *Biophys. J.* **1995**, *68*, 1145−1151.
(80) Rehm, D.; Weller, A. *Isr. J. Chem.* **1970**, *8*, 259−271.
(81) Brunschwig, B. S.; Ehrenson, S.; Sutin, N. *J. Phys. Chem.* **1986**, *90*, 3657−3665.
(82) Sutin, N.; Brunschwig, B. S.; Creutz, C.; Winkler, J. R. *Pure Appl. Chem.* **1988**, *60*, 1817−1830.
(83) Worthington, P.; Hambright, P.; Williams, R. F. X.; Reid, J.; Burnham, C.; Shamim, A.; Turay, J.; Bell, D. M.; Kirkland, R.; Little, R. G.; Datta-Gupta, N.; Eisner, U. *J. Inorg. Biochem.* **1980**, *12*, 281−291.
(84) Pasternack, R. F.; Gibbs, E. J. *Metal Ions Biol. Syst.* **1996**, *33*, 367−397.
(85) Carvlin, M. J.; Fiel, R. J. *Nucl. Acids Res.* **1983**, *11*, 6121−6139.
(86) Gibbs, E. J.; Tinoco, I., Jr.; Maestre, M. F.; Ellinas, P. A.; Pasternack, R. F. *Biochem. Biophys. Res. Commun.* **1988**, *157*, 350−358.
(87) Hudson, B. P.; Sou, J.; Berger, D. J.; McMillin, D. R. *J. Am. Chem. Soc.* **1992**, *114*, 8997−9002.
(88) Pasternack, R. F.; Bustamante, C.; Collings, P. J.; Giannetto, A.; Gibbs, E. J. *J. Am. Chem. Soc.* **1993**, *115*, 5393−5399.
(89) Mukundan, N. E.; Pethö, G.; Dixon, D. W.; Kim, M. S.; Marzilli, L. G. *Inorg. Chem.* **1994**, *33*, 4676−4687.
(90) Mukundan, N. E.; Pethö, G.; Dixon, D. W.; Marzilli, L. G. *Inorg. Chem.* **1995**, *34*, 3677−3687.
(91) McClure, J. E.; Baudouin, L.; Mansuy, D.; Marzilli, L. G. *Biopolymers* **1997**, *42*, 203-217.
(92) Anderson, C. F.; Record, M. T., Jr. *Annu. Rev. Phys. Chem.* **1995**, *46*, 657−700.
(93) Gray, T. A.; Yue, K. T.; Marzilli, L. G. *J. Inorg. Biochem.* **1991**, *41*, 205−219.
(94) Kuroda, R.; Takahashi, E.; Austin, C. A.; Fisher, L. M. *FEBS Lett.* **1990**, *262*, 293−298.
(95) Marzilli, L. G.; Pethö, G.; Lin, M.; Kim, M. S.; Dixon, D. W. *J. Am. Chem. Soc.* **1992**, *114*, 7575−7577.
(96) Lipscomb, L. A.; Zhou, F. X.; Presnell, S. R.; Woo, R. J.; Peek, M. E.; Plaskon, R. R.; Williams, L. D. *Biochemistry* **1996**, *35*, 2818−2823.
(97) Pasternack, R. F.; Garrity, P.; Ehrlich, B.; Davis, C. B.; Gibbs, E. J.; Orloff, G.; Giartosio, A.; Turano, C. *Nucl. Acids Res.* **1986**, *14*, 5919−5931.
(98) Steullet, V.; Dixon, D. W. *J. Inorg. Biochem.*, in press.
(99) Kano, K.; Takei, M.; Hashimoto, S. *J. Phys. Chem.* **1990**, *94*, 2181−2187.
(100) Liu, Y. X.; Koningstein, J. A. *J. Phys. Chem.* **1993**, *97*, 6155−6160.
(101) Kano, K.; Miyake, T.; Uomoto, K.; Sate, T.; Ogawa, T.; Hashimoto, S. *Chem. Lett.* **1983**, 1867−1870.
(102) Brookfield, R. L.; Ellul, H.; Harriman, A. *J. Photochem.* **1985**, *31*, 97−103.
(103) Kano, K.; Nakajima, T.; Takei, M.; Hashimoto, S. *Bull. Chem. Soc. Jpn.* **1987**, *60*, 1281−1287.
(104) Liu, Y. X.; Koningstein, J. A.; Yevdokimov, Y. *Can. J. Chem.* **1991**, *69*, 1791−1795.
(105) Kemnitz, K.; Sakagushi, T. *Chem. Phys. Lett.* **1992**, *196*, 497−503.
(106) Yonemoto, E. H.; Saupe, G. B.; Schmehl, R. H.; Hubig, S. M.; Riley, R. L.; Iverson, B. L.; Mallouk, T. E. *J. Am. Chem. Soc.* **1994**, *116*, 4786−4795.
(107) Carvlin, M. J.; Datta-Gupta, N.; Fiel, R. J. *Biochem. Biophys. Res. Commun.* **1982**, *108*, 66−73.
(108) Bustamante, C.; Gurrieri, S.; Pasternack, R. F.; Purrello, R.; Rizzarelli, E. *Biopolymers* **1994**, *34*, 1099−1104.
(109) Schneider, H.-J.; Wang, M. *J. Org. Chem.* **1994**, *59*, 7473−7478.